

Theoretical Insight into $\text{Sc}_2\text{O}@\text{C}_{84}$: Interplay between Small Cluster and Large Carbon Cage

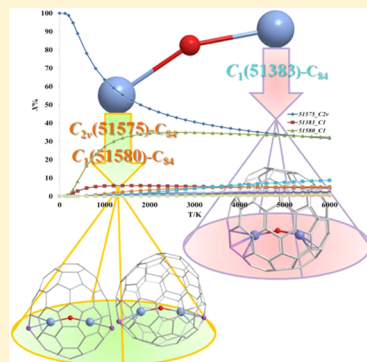
Yi-Jun Guo,^{†,‡} Xiang Zhao,^{*,†,‡} Pei Zhao,^{†,‡} and Tao Yang[§]

[†]Institute for Chemical Physics & Department of Chemistry, MOE Key Laboratory for Non-equilibrium Condensed Matter and Quantum Engineering, School of Science and [‡]State Key Laboratory of Electrical Insulation and Power Equipment, Xi'an Jiaotong University, Xi'an 710049, China

[§]Institute for Molecular Science, Okazaki 444-8585, Japan

Supporting Information

ABSTRACT: Very recently, a series of endohedral fullerenes $\text{Sc}_2\text{O}@\text{C}_{2n}$ ($n = 35–47$) were facilely produced. However, only two of them have been further characterized so far. Theoretically, we studied another scandium oxide endohedral fullerene without any characterizations, $\text{Sc}_2\text{O}@\text{C}_{84}$, which is the second most-abundant species in terms of relative heights of all mass spectrum peaks. Two thermodynamically stable isomers with isolated pentagon rule-obeying cages were found, namely, $\text{Sc}_2\text{O}@\text{C}_{2v}(51575)-\text{C}_{84}$ and $\text{Sc}_2\text{O}@\text{C}_1(51580)-\text{C}_{84}$. This is the first case that an endohedral fullerene containing the $\text{C}_{2v}(51575)-\text{C}_{84}$ cage acts as the lowest-energy isomer, and it is the first report of a clusterfullerene containing the $\text{C}_1(51580)-\text{C}_{84}$ cage. The endohedral Sc_2O cluster can keep its ideal structure after encapsulation, while both C_{84} cages have deformed dramatically. Orbital analysis suggests that nucleophilic and oxidation reactions of both isomers should take place on the cage, while regioselectivity of $\text{Sc}_2\text{O}@\text{C}_{2v}(51575)-\text{C}_{84}$ and $\text{Sc}_2\text{O}@\text{C}_1(51580)-\text{C}_{84}$ is different due to their different characteristics of the highest occupied orbital distribution. Two-dimensional electron localization function and Laplacian of electron density maps unambiguously indicate strong electrostatic interactions exist between one scandium atom and the oxygen one. Meanwhile, overlaps of occupied metal atom orbitals and the cage ones along with Mayer bond order analysis identify that covalent interactions between a scandium atom and each C_{84} cage cannot be neglected. At last, ^{13}C NMR, UV-vis-NIR, and IR spectra of both $\text{Sc}_2\text{O}@\text{C}_{84}$ isomers were simulated theoretically. Because of their structural difference, all spectra between two isomers are significantly divergent. Consequently, these spectra are helpful to distinguish $\text{Sc}_2\text{O}@\text{C}_{2v}(51575)-\text{C}_{84}$ and $\text{Sc}_2\text{O}@\text{C}_1(51580)-\text{C}_{84}$ in further experimental characterizations.



INTRODUCTION

Endohedral metallofullerenes (EMFs)¹ are fullerenes with metals or a metal cluster inside. After the encapsulation, electronic properties can be changed compared with those of the same pristine fullerene, and plenty of novel but unstable fullerene cages can be stabilized and separable after the encapsulation. For example, the $\text{C}_{2v}(4059)-\text{C}_{66}$ cage, which contains two unsaturated linear triquinanes, can be stabilized by two scandium ions nestled between those two moieties.² Moreover, a nonclassical C_{80} cage that contains a heptagonal ring can be stabilized by a LaSc_2N cluster, forming stable $\text{LaSc}_2\text{N}@\text{C}_8(\text{hept})-\text{C}_{80}$ metallofullerene.³ Note that those encapsulated metal clusters such as Sc_2 and LaSc_2N mentioned above cannot exist alone, so endohedral metallofullerenes provide possibilities for the study on special metal–metal/nonmetal interactions. A representative example indicates that there is a non-nuclear attractor among three yttrium atoms in the genuine trimetallofullerene $\text{Y}_3@\text{I}_h-\text{C}_{80}$, which can only exist among the lightest lithium atoms under normal circumstances.⁴ Consequently, EMFs have attracted board attention globally, and a series of them has been synthesized, isolated, and characterized. They also show anticipated applications in many

areas, such as biomedicine, organic photovoltaics, superconductors, nanomemory device, and ferroelectric materials.^{5–10} At the same time, these potential applications further promote the development of EMFs.

The $\text{Sc}_3\text{N}@\text{I}_h-\text{C}_{80}$ metallofullerene was isolated and structurally characterized by Stevenson et al. in 1999,¹¹ proclaiming the birth of cluster EMFs. Since then, a variety of metal clusters can be encapsulated inside different fullerene cages. Until now, besides the first discovered metal nitride cluster-EMFs, cluster EMFs also include metal carbide ones,^{12–14} metal sulfide ones,^{15–17} metal cyanide ones,^{17–21} metal oxide ones,^{22–26} and so on. Among them, the recently reported metal oxide EMFs remain to be further studied because metal oxide clusters are protean although their metal atoms are limited to the unique scandium one. Several kinds of confirmed metal oxide clusters include Sc_4O_3 ,²² Sc_4O_2 ,²³ and Sc_2O .^{24,25} It should also be pointed out that an even larger eight-atom cubane oxide M_4O_4 cluster can also be encapsulated inside other middle-sized

Received: July 29, 2015

Revised: September 17, 2015

Published: September 21, 2015

fullerenes, proposed by Poblet et al. after making a comparison with the characterized $\text{Sc}_4\text{O}_3@\text{C}_{80}$ metallofullerene.²⁶ This is quite different from sulfide clusterfullerenes. It is known that oxygen and sulfur are in the same group of the periodic table, while M_2S ($M = \text{metal}$) is the only discovered cluster encapsulated in fullerene cages. Those Sc_4O_3 and Sc_4O_2 clusters can only be captured in the $I_h(7)-\text{C}_{80}$ cage in terms of existing reports.^{22,23} Although the Sc_2O and Sc_2S units are valence isoelctronic, only one $\text{Sc}_2\text{O}@\text{C}_{82}$ was found in the same progress of making $\text{Sc}_4\text{O}_2@\text{C}_{80}$ and $\text{Sc}_4\text{O}_3@\text{C}_{80}$ rather than a series of discandium oxide EMFs²⁴ like $\text{Sc}_2\text{S}@\text{C}_{2n}$ ($2n = 68-100$).^{27,28}

Very recently, an extensive family of discandium oxide EMFs with cage size ranging from C_{70} to C_{94} was synthesized by introducing CO_2 as the oxygen source.²⁵ At the same time, a series of experimental characterizations combined with theoretical computations have been performed to the smallest identified discandium oxide fullerene, $\text{Sc}_2\text{O}@\text{C}_{70}$. To the best of our knowledge, this is the first report on a series of $\text{Sc}_2\text{O}@\text{C}_{2n}$ metallofullerenes. Later, crystallographic and computational studies were performed on a somewhat minor production, $\text{Sc}_2\text{O}@\text{C}_{76}$,²⁹ while there are still no detailed experimental or theoretical analyses on other reported $\text{Sc}_2\text{O}@\text{C}_{2n}$ species, including $\text{Sc}_2\text{O}@\text{C}_{84}$. In terms of the relative height of $\text{Sc}_2\text{O}@\text{C}_{2n}$ series' mass spectrum peaks illustrated in Feng's paper,²⁵ $\text{Sc}_2\text{O}@\text{C}_{84}$ is the second most-abundant species compared with the highest peak representing the $\text{Sc}_2\text{O}@\text{C}_{82}$ one. Consequently, besides $\text{Sc}_2\text{O}@\text{C}_{82}$ and $\text{Sc}_2\text{O}@\text{C}_{76}$, of which single crystals have been obtained, $\text{Sc}_2\text{O}@\text{C}_{84}$ is another good representative for revealing characteristics of dimetal oxide metallofullerenes.

Until now, several kinds of C_{84} -based EMFs have been well-studied, including monometal,³⁰⁻³² dimetal carbide cluster,³³⁻³⁵ trimetal nitride cluster,³⁶⁻³⁹ and dimetal sulfide cluster⁴⁰ metallofullerenes. Totally seven C_{84} cages can be stabilized by encapsulation, and two of them violate the isolated pentagon rule (IPR).⁴¹ Interestingly, both $\text{Sc}_2\text{C}_2@\text{C}_{84}$ and $\text{M}_2\text{C}_2@\text{C}_{84}$ ($M = \text{Y}$ and Gd) belong to carbide clusterfullerenes with a formal four-electron transfer from metal cluster to C_{84} , but their cage structures are quite divergent³³⁻³⁵ due to the size difference of a triscandium nitride cluster and a triyttrium/gadolinium one. Considering the encapsulation of a quite small discandium oxide cluster in a relatively large C_{84} cage, it is still interesting and meaningful to investigate its physical and chemical properties as well as metal–cage interactions of $\text{Sc}_2\text{O}@\text{C}_{84}$. Obviously, thermodynamically favorable isomers should be confirmed at first. Notably, three isomers of $\text{Sc}_2\text{S}@\text{C}_{76}$ compete in the temperature region of fullerene formation,⁴² while only one $\text{Sc}_2\text{O}@\text{C}_{76}$ isomer with the $T_d(19151)-\text{C}_{76}$ cage²⁹ is overwhelming. Accordingly, it can be expected that properties of $\text{Sc}_2\text{O}@\text{C}_{84}$ are different from those of the previously reported $\text{Sc}_2\text{S}@\text{C}_{84}$ as well as other kinds of C_{84} -based metallofullerenes.

Herein, we report quantum chemistry combined with statistical thermodynamics investigations on the geometry and electronic structure of dimetal oxide clusterfullerene $\text{Sc}_2\text{O}@\text{C}_{84}$. We demonstrate that two IPR-obeying cages are utilized to encapsulate a discandium oxide cluster. Meanwhile, frontier molecular orbital analysis and bonding natures, as well as electronic absorption, infrared, and ^{13}C NMR spectra were theoretically investigated. The purpose of this paper not only aims to the cage structure and the arrangement of discandium oxide cluster but also expands the understanding of bonding

natures as well as physical and chemical properties of C_{84} -based EMFs. We hope all theoretical characterizations can provide useful assistance for future experimental identification of $\text{Sc}_2\text{O}@\text{C}_{84}$ isomers.

■ COMPUTATIONAL DETAILS

Previous studies on metallofullerenes containing a Sc_2X ($X = \text{O}$ or S) cluster have shown a formal four-electron transfer^{16,24,27,28} from the metal cluster to the carbon cage. However, some experimental and computational evidence indicates that divalent Sc ions are also reasonable in some EMFs.⁴³⁻⁴⁵ Thus, before determining candidates for the encapsulation of a discandium oxide cluster, both di- and tetra- C_{84} anions were taken into account. In terms of a previous work,³⁴ we chose 15 tetra- C_{84} anions including the top-eight ones obeying IPR, the top-six ones with one adjacent pentagon pair (APP), and the lowest-energy one with two APPs. As for di- C_{84} anions, those isomers with the number of APPs less than four were first screened by AM1 method. Then, all isomers with relative energies less than 35 kcal·mol⁻¹ were reoptimized at the hybrid density functional B3LYP⁴⁶⁻⁴⁸ with the split-valence d-polarized 6-31G(d) basis set. Later, those top-six IPR and top-five one-APP cages were selected for the study of endohedral a discandium oxide cluster. Totally, 23 C_{84} cages were initially considered. Relative energy sequences of di- C_{84} anions screened at AM1 and B3LYP/6-31G(d) level are listed in Tables S1 and S2 of Supporting Information, respectively.

Geometry optimizations of $\text{Sc}_2\text{O}@\text{C}_{84}$ were performed with M06-2X⁴⁹ density functional, and the Lanl2dz⁵⁰ basis set with the corresponding effective core potential was applied on scandium atoms. Three basis sets, namely, 3-21G*, 6-31G(d), and 6-311G(d), were used for C and O in different steps of optimization. To gain the global minimum of each $\text{Sc}_2\text{O}@\text{C}_{84}$ isomer on the potential energy surface, 8 to 12 different orientations of the endohedral Sc_2O cluster were taken into consideration. Two relative energy sequences of those favorable configurations optimized at M062X/6-31G(d) ~ Lanl2dz and M062X/6-311G(d) ~ Lanl2dz levels, respectively, are listed in Table 1. A detailed description on the process of selecting promising $\text{Sc}_2\text{O}@\text{C}_{84}$ isomers is provided in the Supporting Information (please see Section II). Finally, to confirm that the relative energy order of $\text{Sc}_2\text{O}@\text{C}_{84}$ is reasonable, two other density functionals B3PW91^{47,51} and PBEPBE⁵² were performed on eight isomers with 6-311G(d) ~ Lanl2dz basis sets for nonmetal atoms and scandium ones, respectively (please see Section III of Supporting Information for details).

All stationary points were verified as minima by vibrational frequency analysis at M06-2X/6-31G(d) ~ Lanl2dz level of theory. On the basis of the frequency analysis, rotational-vibrational partition functions also could be obtained, and then the molar fraction of each $\text{Sc}_2\text{O}@\text{C}_{84}$ candidate as a function of temperature was computed, which combined relative energy and entropic contributions.⁵³ Notably, a series of single-crystal X-ray diffraction (XRD) characterizations have unambiguously confirmed that entropy effect also plays an important role on stabilization of metal clusterfullerenes.^{24,29,34,35}

The UV-vis-NIR simulation on two thermodynamic stable $\text{Sc}_2\text{O}@\text{C}_{84}$ isomers were performed by time-dependent (TD) DFT calculations utilizing the polarizable continuum model (PCM)⁵⁴ with B3LYP density functional and 6-31G(d) ~ Lanl2dz basis sets. Toluene was selected as the solvent. The ^{13}C NMR spectrum simulations employing the gauge including atomic orbital (GIAO) method were also produced by the

Table 1. Relative Energies (in $\text{kcal}\cdot\text{mol}^{-1}$) and HOMO–LUMO Gaps (in eV) of $\text{Sc}_2\text{O}@C_{82}$ Isomers at M06-2X/6-31G(d) ~ Lanl2dz and M06-2X/6-311G(d) ~ Lanl2dz Levels of Theory

spiral no.	Fowler No.	cage symmetry	M06-2x/6-31G(d) ~ Lanl2dz		M06-2x/6-311G(d) ~ Lanl2dz	
			relative energy	gap	relative energy	gap
S1575	7	C_{2v}	0.0	3.14	0.0	3.12
S1383		C_1	1.1	3.23	0.9	3.22
S1580	12	C_1	2.1	3.13	2.1	3.10
S1589	21	D_2	3.9	2.80	4.6	2.78
S1483		C_1	4.3	3.19	4.0	3.18
S1578	10	C_s	4.9	2.84	5.3	2.81
S1482		C_1	5.1	2.72	5.2	2.71
S1591	23	D_{2d}	8.0	2.37	8.4	2.36
S1365		C_s	10.2	2.70	10.1	2.69
S1583	15	C_s	10.5	2.44	10.9	2.42
S1590	22	D_2	11.4	2.70	11.2	2.66
S1550		C_s	11.6	3.13	11.6	3.12
S1581	13	C_2	13.3	2.47	13.3	2.46
S1546		C_s	15.1	3.07	14.9	3.06
S1499		C_1	18.6	2.34		
S1539		C_1	19.3	2.61		
S1579	11	C_2	20.5	2.54		
S1519		C_s	28.0	2.86	27.9	2.85

M06-2X functional theory with the Lanl2dz basis set for scandium atoms and a larger 6-311G(2d) basis set for C and O. Theoretical chemical shift values were calibrated to the observed C_{60} line (142.15 ppm).⁵⁵ All DFT calculations mentioned above were performed by Gaussian 09 program.⁵⁶

RESULTS AND DISCUSSION

Thermodynamic Stabilities of $\text{Sc}_2\text{O}@C_{84}$ Series. Although the lowest-energy isomer optimized at M06-2X/3-21G* ~ Lanl2dz level possesses the non-IPR C_1 (S1383)- C_{84} cage (please see Table S5 in Supporting Information), optimization at another four levels of theory suggests that a discandium oxide cluster captured by the C_{2v} (S1575)- C_{84} exhibits the lowest energy among all $\text{Sc}_2\text{O}@C_{84}$ isomers, as shown in Table 1 as well as Tables S9 and S10. To the best of our knowledge, it is the first time to discover that the lowest-energy C_{84} -based endohedral fullerene possesses the C_{2v} (S1575)- C_{84} cage. Interestingly, the Sc_2O cluster shows important contributions to the stabilization of C_{84} cages violating IPR. There are as many as five non-IPR $\text{Sc}_2\text{O}@C_{84}$ isomers of which relative energy is less than 15 $\text{kcal}\cdot\text{mol}^{-1}$. Reoptimizations at M06-2X/6-311G(d) ~ Lanl2dz level have further confirmed the energy sequence of the top three isomers. The sequence change of the following four isomers is acceptable because of the extremely narrow energy gaps between $\text{Sc}_2\text{O}@D_2$ (S1589)- C_{84} and $\text{Sc}_2\text{O}@C_1$ (S1483)- C_{84} as well as $\text{Sc}_2\text{O}@C_s$ (S1578)- C_{84} and $\text{Sc}_2\text{O}@C_1$ (S1482)- C_{84} isomers. Meanwhile, the highest occupied molecular orbital (HOMO)–the lowest unoccupied molecular orbital (LUMO) gaps calculated at two levels are comparable. All isomers show fairly large gaps, indicating substantial kinetic stabilities. Remarkably, a formal four-electron transfer takes place from both Sc_2O and Y_2C_2 clusters to C_{84} cages in $\text{Sc}_2\text{O}@C_{84}$ and $\text{Y}_2\text{C}_2@C_{84}$ ³⁴ isomers, but their lowest-energy isomers own two different cages. Consequently, different endohedral metal

clusters have different influences on the choice of fullerene cage isomer.

Notably, a relatively large C_{84} cage encapsulates a small Sc_2O cluster forming the endohedral metallofullerene $\text{Sc}_2\text{O}@C_{84}$. Consequently, one can expect divergent orientations of a discandium oxide cluster in each carbon cage. The same cage structure with different arrangements of Sc_2O cluster can have noticeable different potential energies. We analyzed at least eight different pristine orientations of the Sc_2O moiety inside 18 C_{84} isomers including C_{2v} (S1575), C_1 (S1580), and C_1 (S1383). Some pristine orientations of the internal cluster turn into the same final orientation after geometry optimization. For example, as shown in Table S4, nine orientations of the captured cluster were analyzed for isomer $\text{Sc}_2\text{O}@C_1$ (S1482)- C_{84} , while four of them with serial number of 5, 3, 1, and 4 possess the same configuration after geometry optimization. They have similar energy levels of HOMO and LUMO. In general, it can be inferred from Table S4 that motion of Sc_2O inside different C_{84} cages may be hindered. For Sc_2O encapsulated in C_{2v} (S1575)- C_{84} , C_1 (S1383)- C_{84} , and C_1 (S1580)- C_{84} cages, only one configuration can be found as the global minimum on their potential energy surfaces. This is quite different from the situation of three $\text{Sc}_2\text{O}@C_{82}$ isomers C_s (6), C_{3v} (8), and C_{2v} (9). Sc_2O can rotate quite freely inside C_{82} cages. Compared with C_{82} , those C_{84} cages possess larger cavity. As a result, when a Sc_2O cluster is encapsulated by C_{2v} (S1575)- C_{84} or C_1 (S1580)- C_{84} cage with specific orientation, it may form strong enough cage-cluster interactions.

Energy gaps of adjacent $\text{Sc}_2\text{O}@C_{84}$ isomers in Table 1 are significantly small. As a result, the potential energy of each isomer at 0 K cannot reflect their real relative stabilities at the temperature region of 500–3000 K, which is the temperature region of EMF formation.⁵⁷ Many cases reported previously^{58–60} show that the relative abundance of EMF isomers with higher energy can surpass the lowest-energy isomer in the EMF formation temperature interval. To confirm which isomers would survive in experimental process, the relationship between molar fractions of each $\text{Sc}_2\text{O}@C_{84}$ candidate and different temperatures in terms of statistic thermodynamics were calculated for all 15 isomers.

As shown in Figure 1, $\text{Sc}_2\text{O}@C_{2v}$ (S1575)- C_{84} is the unique isomer at the temperature of 0 K due to the lowest relative energy. With the increase of temperature, its abundance

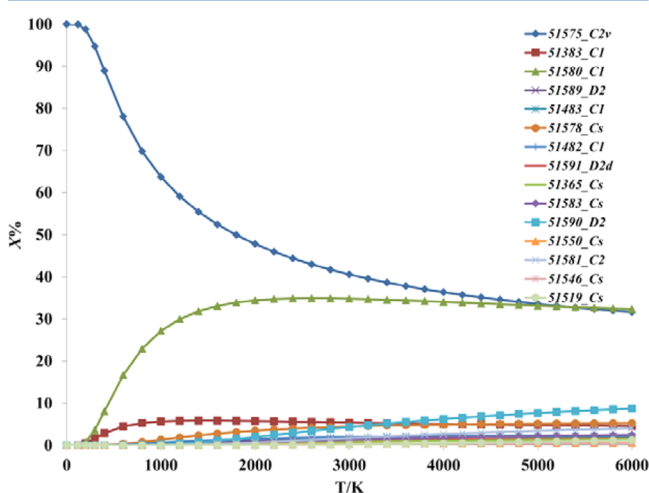


Figure 1. Relative concentrations of 15 low-energy isomers.

decreases gradually. At the same time, the abundance of another structure, $\text{Sc}_2\text{O}@\text{C}_1(51580)\text{-C}_{84}$, rises dramatically, and it catches up with the abundance of $\text{Sc}_2\text{O}@\text{C}_{2v}(51575)\text{-C}_{84}$ after 2500 K. Surprisingly, the second lowest-energy isomer, $\text{Sc}_2\text{O}@\text{C}_1(51383)\text{-C}_{84}$, reaches its maximum abundance at ~ 1500 K, but its molar fraction is still less than 6% with respect to fractions of 52% ($\text{Sc}_2\text{O}@\text{C}_{2v}(51575)\text{-C}_{84}$) and 33% ($\text{Sc}_2\text{O}@\text{C}_1(51580)\text{-C}_{84}$) at the same temperature. It has been proved unambiguously that a diyttrium or digadolinium carbide cluster can stabilize the $\text{C}_1(51383)\text{-C}_{84}$ cage. Y_2C_2 ³⁴ and Gd_2C_2 ³⁵ clusters together with the Sc_2O one transfer four electrons to a C_{84} cage formally, but they have different selectivity to fullerene cages. Other $\text{Sc}_2\text{O}@\text{C}_{84}$ isomers have no obvious contributions in the whole temperature region although they also possess somewhat low energies. Figure 1 unambiguously uncovers that the mass spectrum signal of $\text{Sc}_2\text{O}@\text{C}_{84}$ includes two isomers, $\text{Sc}_2\text{O}@\text{C}_{2v}(51575)\text{-C}_{84}$ and $\text{Sc}_2\text{O}@\text{C}_1(51580)\text{-C}_{84}$, and the former is a relatively main production. This observation can partially explain why the abundance of $\text{Sc}_2\text{O}@\text{C}_{84}$ is even larger than that of the recently isolated $\text{Sc}_2\text{O}@\text{C}_{76}$ isomers. Theoretical calculations²⁹ show that $\text{Sc}_2\text{O}@\text{T}_d(19151)\text{-C}_{76}$ is the only thermodynamically stable isomer in whole temperature region.

It should be pointed out that the $\text{C}_{2v}(51575)\text{-C}_{84}$ cage seldom can be stabilized by endohedral metal atoms or a metal cluster. Before the discandium oxide clusterfullerene studied at present, this cage might survive just when a discandium sulfide cluster⁴⁰ is encapsulated in it. Because of its high relative energy, the thermodynamic superiority of $\text{Sc}_2\text{S}@\text{C}_{2v}(51575)\text{-C}_{84}$ appears only at high-temperature regions. Consequently, unlike the $\text{Sc}_2\text{O}@\text{C}_{2v}(51575)\text{-C}_{84}$ as a main product here, the quantity of $\text{Sc}_2\text{S}@\text{C}_{2v}(51575)\text{-C}_{84}$ should be minor. As for those characterized EMFs containing the $\text{C}_1(51580)\text{-C}_{84}$ cage, all of them belong to monometallofullerenes. Herein, this is the first evidence that the $\text{C}_1(51580)\text{-C}_{84}$ cage can also be stabilized by a metal cluster. It is the first time to discover a final product of EMF containing a combination of $\text{C}_{2v}(51575)\text{-C}_{84}$ and $\text{C}_1(51580)\text{-C}_{84}$ cages. Indeed, new endohedral oxide metallofullerenes broaden our horizon on fullerene science.

Geometric Peculiarities and Binding Energies of Two Favorable $\text{Sc}_2\text{O}@\text{C}_{84}$ Isomers. As depicted in Table S4 of Supporting Information, only one favorable structure is found for both $\text{Sc}_2\text{O}@\text{C}_{2v}(51575)\text{-C}_{84}$ and $\text{Sc}_2\text{O}@\text{C}_1(51580)\text{-C}_{84}$ molecules. Their configurations are displayed in Figure 2. V-shaped discandium oxide clusters are encapsulated in both cages with large obtuse $\text{Sc}-\text{O}-\text{Sc}$ angles, which are 156.0° and 159.0° , respectively. The degrees of these angles are comparable with that for $\text{Sc}_2\text{O}@\text{C}_s(6)\text{-C}_{82}$ (156.6°)²⁴ but dramatically more obtuse than that for $\text{Sc}_2\text{O}@\text{C}_2(7892)\text{-C}_{70}$ (139.23°)²⁵ or for $\text{Sc}_2\text{O}@\text{T}_d(19151)\text{-C}_{76}$ (146.9°).²⁹ Consequently, the large cavities of $\text{C}_{2v}(51575)\text{-C}_{84}$ and $\text{C}_1(51580)\text{-C}_{84}$ cages can provide enough space for the capture of a Sc_2O cluster without any nanoscale compression.⁶¹ It can be further inferred that it is the ideal structure of a Sc_2O cluster when it is trapped in the $\text{C}_{2v}(51575)\text{-C}_{84}$, $\text{C}_1(51580)\text{-C}_{84}$, and $\text{C}_s(6)\text{-C}_{82}$ cages because no obvious $\text{Sc}-\text{O}-\text{Sc}$ angle changes take place with the increase of carbon cage from C_{82} to C_{84} . The shortest $\text{Sc}-\text{cage}$ distances in $\text{Sc}_2\text{O}@\text{C}_{2v}(51575)\text{-C}_{84}$ and $\text{Sc}_2\text{O}@\text{C}_1(51580)\text{-C}_{84}$ molecules are $2.251/2.255$ Å and $2.254/2.272$ Å, respectively. All of them are comparable but somewhat larger than those in $\text{Sc}_2\text{C}_2@\text{D}_{2d}(23)\text{-C}_{84}$ ³³ because the size of a Sc_2O cluster is smaller than that of a Sc_2C_2 cluster.

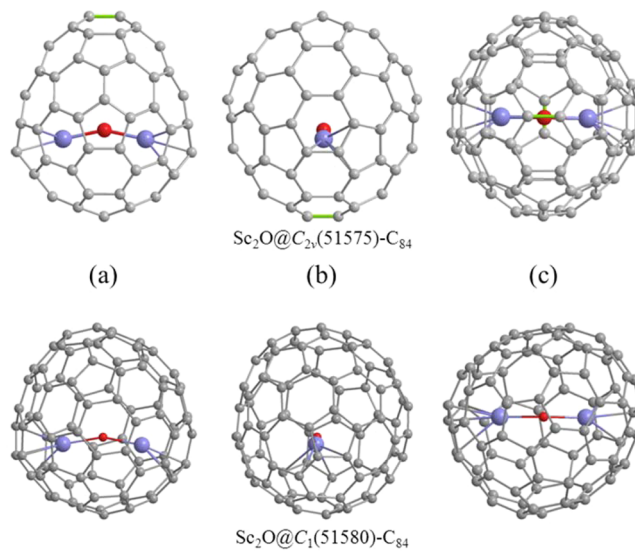


Figure 2. Main view (a), side view (b), and top view (c) of $\text{Sc}_2\text{O}@\text{C}_{2v}(51575)\text{-C}_{84}$ and $\text{Sc}_2\text{O}@\text{C}_1(51580)\text{-C}_{84}$. Carbon, oxygen, and scandium atoms are colored by gray, red, and violet, respectively. Those two C–C bonds perpendicularly bisected by the C_{2v} axis of $(51575)\text{-C}_{84}$ cage are highlighted by green color.

Although two thermodynamically stable $\text{Sc}_2\text{O}@\text{C}_{84}$ isomers are similar on some geometric parameters, they still differ due to the difference of two C_{84} cages. The discandium cluster in $\text{C}_{2v}(51575)\text{-C}_{84}$ cage possess two equal $\text{Sc}-\text{O}$ distances with the number of 1.89 Å, so the V-shaped cluster belongs to the same C_{2v} symmetry as the carbon cage. Furthermore, as shown in Figure S2 of Supporting Information, the symmetry planes and C_2 axis of the cage and metal cluster are coincident, resulting that the $\text{Sc}_2\text{O}@\text{(51575)}\text{-C}_{84}$ keeps the C_{2v} symmetry of its pristine carbon cage. Thus, it is obvious that two shortest $\text{Sc}-\text{cage}$ distances are almost equal due to the equivalence of those two carbon atoms. There are no equivalent carbon atoms on the $(51580)\text{-C}_{84}$ cage due to its C_1 symmetry, leading to different chemical environment on different carbon atoms. As a result, those two shortest $\text{Sc}-\text{cage}$ distances are a bit different. At the same time, two $\text{Sc}-\text{O}$ distances are also not isometric, which are 1.88 and 1.93 Å with homologous $\text{Sc}-\text{cage}$ distances of 2.272 and 2.254 Å. Interestingly, a longer $\text{Sc}-\text{cage}$ distance corresponds to a short one from the same scandium to the oxygen atom of Sc_2O cluster.

To further clarify the influence on fullerene cage caused by endohedral metal cluster, we compared geometric changes of two cages along with the axis of trapped Sc_2O cluster, as depicted in Figure S3 of Supporting Information. The deformation of $\text{C}_{2v}(51575)\text{-C}_{84}$ and $\text{C}_1(51580)\text{-C}_{84}$ cages reaches as large as 0.18 and 0.29 Å, respectively, in spite of only a small metal cluster inside. The prominent deformation of two cages may be attributed to Coulomb repulsion of two scandium atoms. The obvious deformation of two cages is quantified as large cage deformation energies, which are ~ 30 kcal·mol⁻¹ (please see Table S11 for details). Interestingly, the $\text{C}_1(51580)\text{-C}_{84}$ cage has more distinct deformation, but its deformation energy is a bit smaller than that of the $\text{C}_{2v}(51575)\text{-C}_{84}$ cage. Therefore, it seems no quantitative relationship between deformation quantity and deformation energy. However, it is undisputed that the cage deformation stemming from endohedral a discandium cluster decreases stabilities of both cages.

Since the endohedral process decreases the stability of a carbon cage, an open question is how to explain that $\text{Sc}_2\text{O}@\text{C}_{84}$ can be stable existence. To answer it, we calculated binding energies of $\text{Sc}_2\text{O}@\text{C}_{2v}(51575)\text{-C}_{84}$, $\text{Sc}_2\text{O}@\text{C}_1(51580)\text{-C}_{84}$, and $\text{Sc}_2\text{O}@\text{C}_1(51383)\text{-C}_{84}$, including basis set superposition error (BSSE) corrections. As shown in Table S11, both isomers possess a dramatically negative binding energy, indicating that both structures have enough bonding strength to keep endohedral configurations. The bonding energy of $\text{Sc}_2\text{O}@\text{C}_{2v}(51575)\text{-C}_{84}$ is 23.4 kcal·mol⁻¹ more negative than that of $\text{Sc}_2\text{O}@\text{C}_1(51580)\text{-C}_{84}$. Thus, because of its lowest-potential energy, excellent rotational-vibrational contributions, and conspicuous negative binding energy, the $\text{Sc}_2\text{O}@\text{C}_{2v}(51575)\text{-C}_{84}$ molecule becomes the most thermodynamically favorable isomer among all $\text{Sc}_2\text{O}@\text{C}_{84}$ species.

Electronic Structures and Bonding Natures of Two Favorable $\text{Sc}_2\text{O}@\text{C}_{84}$ Isomers. Figure 3 presents the HOMO

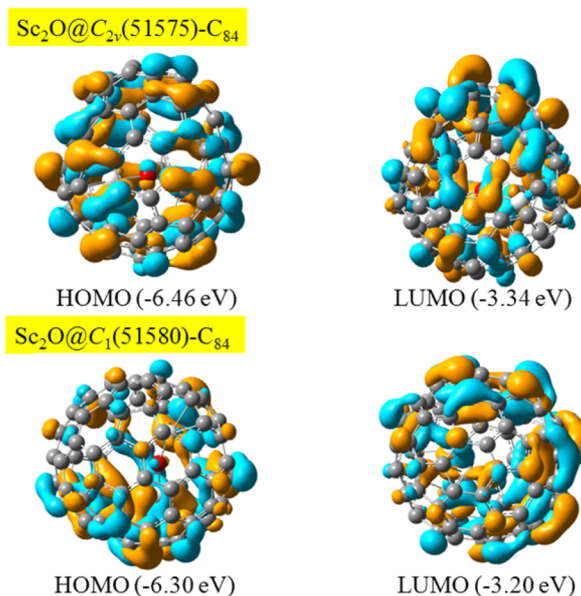


Figure 3. HOMO and LUMO of two thermodynamically favorable $\text{Sc}_2\text{O}@\text{C}_{84}$ isomers.

and the LUMO of $\text{Sc}_2\text{O}@\text{C}_{2v}(51575)\text{-C}_{84}$ and $\text{Sc}_2\text{O}@\text{C}_1(51580)\text{-C}_{84}$, respectively. The HOMO and LUMO of both isomers are mainly contributed by their cage orbitals with small contributions from the discandium oxide cluster. Therefore, either oxidized or reduced reactions involving $\text{Sc}_2\text{O}@\text{C}_{2v}(51575)\text{-C}_{84}$ or $\text{Sc}_2\text{O}@\text{C}_1(51580)\text{-C}_{84}$ molecules should mainly take place on the fullerene cage. Specifically, the HOMO of $\text{Sc}_2\text{O}@\text{C}_1(51580)\text{-C}_{84}$ is mainly adjacent to one scandium atom, suggesting good regioselectivity of nucleophilic and oxidation reactions on the cage. On the contrary, when similar reactions take place on the cage of $\text{Sc}_2\text{O}@\text{C}_{2v}(51575)\text{-C}_{84}$, it is apparent that the regioselectivity is poor due to a symmetrical distribution of HOMO. At the same time, relatively substantial orbital overlaps between metal atomic orbital and cage orbital exist in several occupied frontier orbitals of $\text{Sc}_2\text{O}@\text{C}_1(51580)\text{-C}_{84}$ and $\text{Sc}_2\text{O}@\text{C}_{2v}(51575)\text{-C}_{84}$ (please see Figures 3, S4, and S5 for details), indicating again that the ionic model is oversimplified to EMFs including metal oxide cluster fullerene.

The vertical/adiabatic electron affinity (VEA/AEA) and vertical/adiabatic ionization potential (VIP/AIP) of $\text{Sc}_2\text{O}@\text{C}_{84}$

$\text{C}_{2v}(51575)\text{-C}_{84}$ and $\text{Sc}_2\text{O}@\text{C}_1(51580)\text{-C}_{84}$ were computed conveniently, the results of which are tabulated in Table S12 of Supporting Information. The IP values of both isomers are larger than 6.3 eV, suggesting that they are stable against oxidation. Their EA values are ca. -2.4 eV, which is a bit more negative than that of $\text{Sc}_2\text{S}@\text{C}_2(7892)\text{-C}_{70}$ (-2.03 eV).¹⁶ As a result, they are somewhat easier to be reduced, compared with the C_{70} -based sulfide clusterfullerene. However, if EA values of $\text{Sc}_2\text{O}@\text{C}_{2v}(51575)\text{-C}_{84}$ and $\text{Sc}_2\text{O}@\text{C}_1(51580)\text{-C}_{84}$ are compared with those of $\text{Sc}_2\text{S}@\text{C}_{3v}(8)\text{-C}_{82}$ (-3.61 eV) and $\text{Sc}_2\text{S}@\text{C}_s(6)\text{-C}_{82}$ (-3.69 eV),⁶² both thermodynamically stable $\text{Sc}_2\text{O}@\text{C}_{84}$ isomers are still stable to reduction reactions.

Besides the HOMOs discussed above, a series of other occupied orbitals also were investigated for $\text{Sc}_2\text{O}@\text{C}_{2v}(51575)\text{-C}_{84}$ and $\text{Sc}_2\text{O}@\text{C}_1(51580)\text{-C}_{84}$. Among them, both 88th occupied orbitals (HOMO-179) are delocalized over the captured Sc_2O cluster (please see Figure S6 for details). Therefore, there are both covalent and ionic interactions between a scandium atom and an oxygen one. Notably, the same type of occupied orbital also exists in $\text{Sc}_2\text{S}@\text{C}_{2v}(6073)\text{-C}_{68}$, but it is much closer to the highest occupied orbital, which is the HOMO-8 orbital. Because of the C_{2v} total symmetry of $\text{Sc}_2\text{O}@\text{C}_{2v}(51575)\text{-C}_{84}$, the distribution of its HOMO-179 orbital is symmetric between two scandium atoms, and the oxygen atom locates the center of this orbital. Thus, it can be inferred that the two Sc-O bonds are equivalent. However, the HOMO-179 orbital of $\text{Sc}_2\text{O}@\text{C}_1(51580)\text{-C}_{84}$ is more concentrated between the Sc86 atom and the oxygen one, compared with its distribution between Sc85 and the same oxygen atom. Consequently, the covalent interaction of Sc86-O should be more significant.

Although both the HOMO-8 of $\text{Sc}_2\text{S}@\text{C}_{2v}(6073)\text{-C}_{68}$ and the HOMO-179 of two thermodynamically stable $\text{Sc}_2\text{O}@\text{C}_{84}$ isomers delocalize over the Sc_2X ($\text{X} = \text{O}$ or S) cluster, their spatial distribution characteristics are quite different. As shown in Figure S7, the HOMO-8 of $\text{Sc}_2\text{S}@\text{C}_{2v}(6073)\text{-C}_{68}$ seems like a big π orbital with obvious delocalization, while the HOMO-179 of two thermodynamically stable $\text{Sc}_2\text{O}@\text{C}_{84}$ isomers is more like a σ orbital along with two Sc-O bonds. The difference can be attributed to different electronic properties of an oxygen atom and a sulfur one in spite of the location of same group in periodic table. A sulfur atom is “soft”, which has large polarizability, causing “ductile” valence electron cloud. On the contrary, the $\text{Sc}_2\text{O}@\text{C}_{84}$ molecule is an incorporation of hard scandium and hard oxygen, resulting in that valence electron cloud of Sc and O being localized in the trapped Sc_2O cluster. Therefore, it is reasonable to guess that the interaction between Sc and O is similar to that in $\text{Sc}_2\text{O}@\text{C}_{84}$ when the Sc_2O cluster is captured by other fullerene cages.

To further verify the electrostatic interaction between a scandium atom and an oxygen one for $\text{Sc}_2\text{O}@\text{C}_{2v}(51575)\text{-C}_{84}$ and $\text{Sc}_2\text{O}@\text{C}_1(51580)\text{-C}_{84}$, employing MULTIWFN 3.2.1 program⁶³ we plotted two-dimensional electron localization function(ELF)⁶⁴⁻⁶⁶ and Laplacian of electron density maps of them in the plane determined by two scandium and an oxygen atom, which are illustrated in Figures 4 and 5, respectively. Comparing two illustrations in Figure 4, ELF maps of two $\text{Sc}_2\text{O}@\text{C}_{84}$ isomers are quite similar in the region of discandium oxide cluster. Each atom of the cluster is surrounded by an annular region where the value of ELF is close to 1. At the same time, both values of ELF in the midpoint between a scandium atom and an oxygen one are almost zero. Thus, valence electrons of Sc and O atoms are attracted by their own nucleus

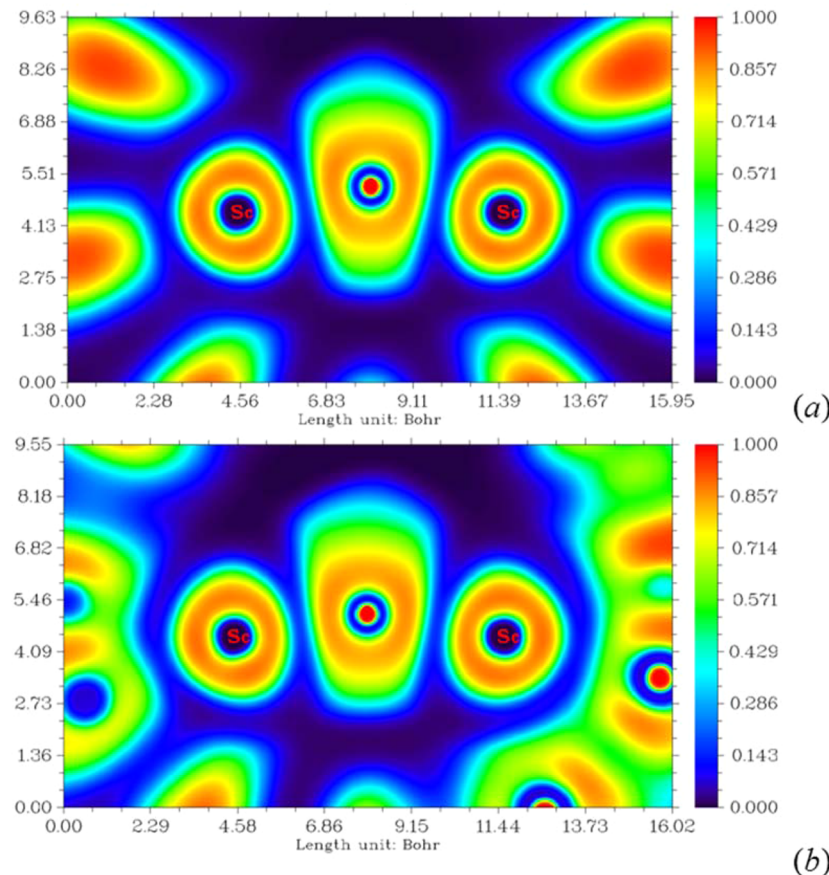


Figure 4. Two-dimensional ELF maps of $\text{Sc}_2\text{O}@C_{2v}(51575)\text{-C}_{84}$ (a) and $\text{Sc}_2\text{O}@C_1(51580)\text{-C}_{84}$ (b) in the plane determined by two scandium and an oxygen atom.

rather than forming shared pairs. As shown in Figure 5, one bond critical points (BCPs) can be found between one scandium atom and the oxygen one for each isomers. Laplacian of electron density at all BCPs and their surrounding areas is positive, indicating that electron density is locally depleted. Consequently, compared with the covalent interaction between scandium and oxygen atoms, electrostatic attractions are still the main interactions between positively charged scandium and the negative oxygen.

To gain a quantificational insight into the covalent interactions of $\text{Sc}_2\text{O}@C_{2v}(51575)\text{-C}_{84}$ and $\text{Sc}_2\text{O}@C_1(51580)\text{-C}_{84}$, still utilizing MULTIWFN 3.2.1 program, we calculated Mayer bond orders⁶⁷ between a scandium atom and the oxygen one as well as one scandium atom and its adjacent carbon atoms. The total bond order between one scandium atom and the whole $C_{2v}(51575)\text{-C}_{84}$ or $C_1(51580)\text{-C}_{84}$ cage were also calculated. Serial numbers of all considered atoms in two $\text{Sc}_2\text{O}@C_{84}$ isomers were shown in Figure 6. As mentioned above, the $\text{Sc}_2\text{O}@C_{2v}(51575)\text{-C}_{84}$ keeps the C_{2v} symmetry of its pristine cage, and the distribution of HOMO-179 orbital is symmetric between two scandium atoms, so two scandium atoms are equivalent. Here, Mayer bond orders of Sc85-O87 and Sc86-O87 are almost the same (please see Table 2). Mayer bond orders of Sc85-O and Sc86-O are 0.7326 and 0.8777, respectively. This is consistent with the fact that the HOMO-179 orbital of $\text{Sc}_2\text{O}@C_1(51580)\text{-C}_{84}$ concentrated between the Sc86 atom and the oxygen one. However, the largest Sc-O bond order (0.8777) is still smaller than that of a Sc-S bond in the $\text{Sc}_2\text{S}@C_{2v}(6073)\text{-C}_{68}$ molecule (1.045 and

1.046¹⁷ for two Sc-S bonds). This further proved that the covalent interaction is less significant in the metallic cluster of a discandium oxide cluster–fullerene compared with that between scandium and sulfur atoms in a sulfide one.

Several bond orders between one scandium atom and its adjacent carbon atoms also were listed in Table 2. All of them are dramatically larger compared with the bond orders between the identical scandium atom and other carbon atoms. Therefore, metal atoms always have the strongest interaction with its adjacent carbon atoms of a fullerene cage. Even so, the maximum Sc-C bond order in either $\text{Sc}_2\text{O}@C_{2v}(51575)\text{-C}_{84}$ or $\text{Sc}_2\text{O}@C_1(51580)\text{-C}_{84}$ (0.1365 and 0.1639) is still less than that in $\text{Sc}_2\text{S}@C_{2v}(6073)\text{-C}_{68}$ (0.211).¹⁷ Unlike the non-IPR $C_{2v}(6073)\text{-C}_{68}$ cage, the IPR $C_{2v}(51575)\text{-C}_{84}$ and $C_1(51580)\text{-C}_{84}$ cages do not need to be strongly coordinated with two scandium atoms to release steric strain. The total bond order between a scandium atom and a C_{84} cage varies from 1.37 to 1.50, which is significantly smaller than that between each Sc atom and the $C_{2v}(6073)\text{-C}_{68}$ cage in the $\text{Sc}_2\text{S}@C_{2v}(6073)\text{-C}_{68}$ molecule. Specifically, the fact that bond orders of Sc85-cage and Sc86-cage in $\text{Sc}_2\text{O}@C_{2v}(51575)\text{-C}_{84}$ are quite similar again demonstrates the equivalence of two scandium atoms.

^{13}C NMR, UV-vis-NIR, and Infrared Spectra of $\text{Sc}_2\text{O}@C_{2v}(51575)\text{-C}_{84}$ and $\text{Sc}_2\text{O}@C_1(51580)\text{-C}_{84}$. Since the holistic symmetry of $\text{Sc}_2\text{O}@C_{2v}(51575)\text{-C}_{84}$ is consist with its pristine $C_{2v}(51575)\text{-C}_{84}$ cage, the EMF possesses 23 nonequivalent carbon atoms. As depicted in Figure S8, four carbon atoms colored by light green have only one equivalent position, while others colored by violet are equivalent with three more carbon

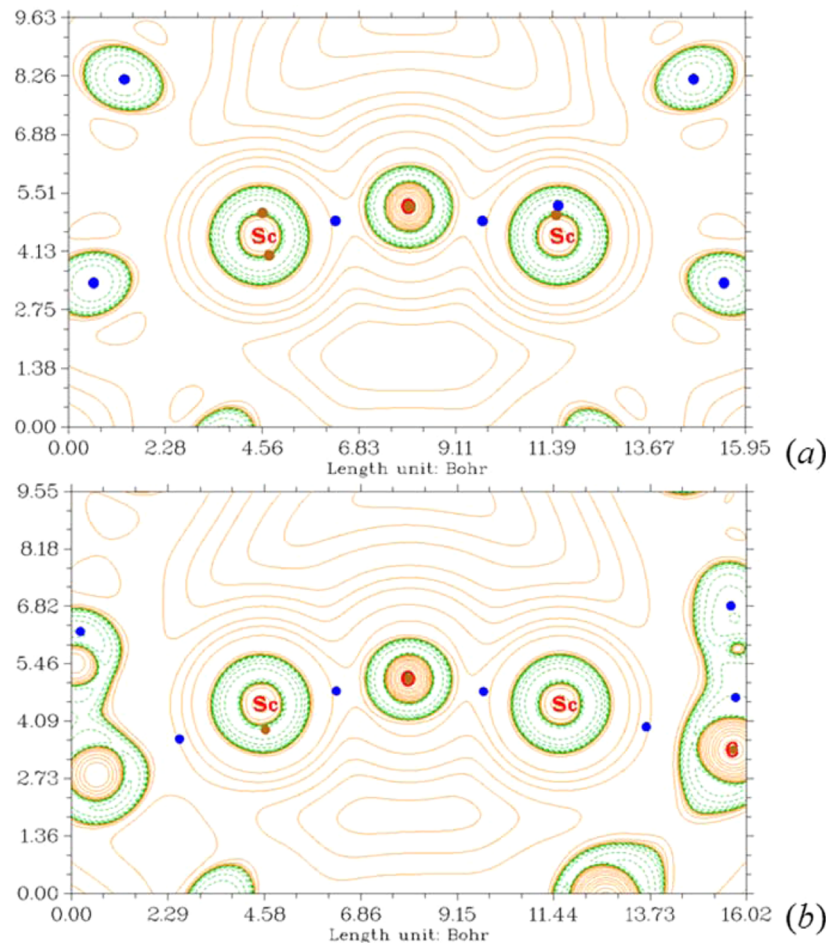


Figure 5. Two-dimensional Laplacian of electron density maps of $\text{Sc}_2\text{O}@\text{C}_{2v}(51575)\text{-C}_{84}$ (a) and $\text{Sc}_2\text{O}@\text{C}_1(51580)\text{-C}_{84}$ (b) in the plane determined by two scandium and an oxygen atom. Green dashed lines and orange full lines represent Laplacian of electron density smaller and larger than zero, respectively. Blue and brown points represent bond critical points (BCP) and nuclear critical points, respectively.



Figure 6. Serial numbers of two scandium atoms, the oxygen atoms, and several carbon atoms adjacent to scandium in $\text{Sc}_2\text{O}@\text{C}_{2v}(51575)\text{-C}_{84}$ and $\text{Sc}_2\text{O}@\text{C}_1(51580)\text{-C}_{84}$.

Table 2. Mayer Bond Orders of Sc–O, Sc–C, and Sc–Cage Interactions, as well as Distances of Corresponding Bonds

	MBO	d (Å)		MBO	d (Å)		
Sc85	C50	0.1327	2.422	Sc85	C40	0.1399	2.399
	C54	0.1357	2.253		C41	0.1472	2.254
	C55	0.1342	2.262		C42	0.1378	2.415
	O87	0.7991	1.892		C56	0.1639	2.271
	cage	1.4347			O87	0.7326	1.928
	C75	0.1336	2.270		cage	1.5042	
	C76	0.1365	2.249		C30	0.1477	2.329
	C77	0.1350	2.407		C31	0.1507	2.272
	O87	0.7975	1.895		C32	0.1262	2.422
	cage	1.4359			O87	0.8777	1.877

atoms. Consequently, totally 23 peaks including 19 full-intensity peaks (four carbons) and four half-intensity peaks (two carbons) are predicted in its ^{13}C NMR spectrum. These peaks range from 124 to 153 ppm. Obviously, there are 84 equal-intensity peaks in the ^{13}C NMR spectrum of $\text{Sc}_2\text{O}@\text{C}_1(51580)\text{-C}_{84}$ due to no equivalent carbon atoms caused by its C_1 symmetry. The span of these peaks, which is in the range from 122 to 159 ppm, seems a bit wider than that of ^{13}C NMR spectrum of $\text{Sc}_2\text{O}@\text{C}_{2v}(51575)\text{-C}_{84}$ simulated at the same level of theory. Clearly, the spectra of two $\text{Sc}_2\text{O}@\text{C}_{84}$ isomers illustrated in Figure 7 are completely different, so the two structures are distinguishable through their ^{13}C NMR spectra. Detailed results of chemical shifts for all nonequivalent carbon atoms were collected in Tables S13 and Table S14 of Supporting Information.

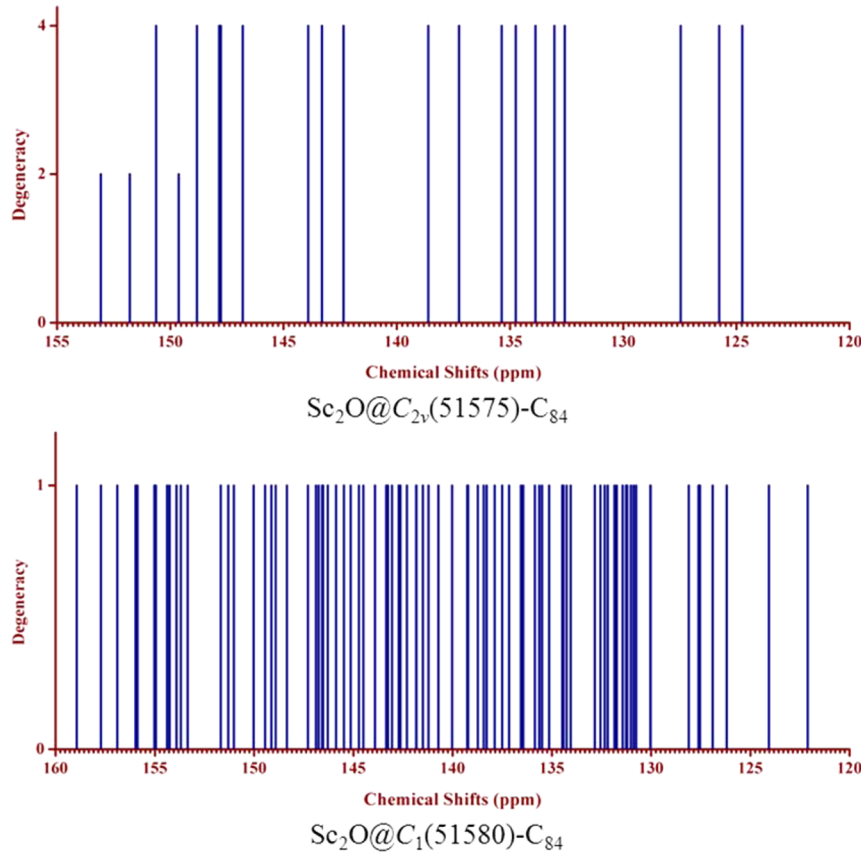


Figure 7. Simulated ^{13}C NMR spectra of $\text{Sc}_2\text{O}@\text{C}_{2v}(51575)\text{-C}_{84}$ and $\text{Sc}_2\text{O}@\text{C}_1(51580)\text{-C}_{84}$.

UV-vis-NIR spectra of $\text{Sc}_2\text{O}@\text{C}_{2v}(51575)\text{-C}_{84}$ and $\text{Sc}_2\text{O}@\text{C}_1(51580)\text{-C}_{84}$ are shown in Figure 8. Although the two structures have identical molecular formula, the characteristic features of their spectra are quite different. There are four strong absorption peaks at 366, 420, 451, and 546 nm along with three broad absorptions at 635, 709, and 922 nm in the spectrum of $\text{Sc}_2\text{O}@\text{C}_{2v}(51575)\text{-C}_{84}$ molecule. As for the $\text{Sc}_2\text{O}@\text{C}_1(51580)\text{-C}_{84}$ structure, as many as 12 absorption peaks can be identified in its spectrum. Compared with corresponding wavelength of $\text{Sc}_2\text{O}@\text{C}_{2v}(51575)\text{-C}_{84}$, all peaks and the absorption onset are more or less red-shifted. Specifically, the first absorption peak of $\text{Sc}_2\text{O}@\text{C}_{2v}(51575)\text{-C}_{84}$ and $\text{Sc}_2\text{O}@\text{C}_1(51580)\text{-C}_{84}$ locates at 922 and 980 nm, corresponding to excitation energies of 1.35 and 1.27 eV, respectively. The first absorption peak of $\text{Sc}_2\text{O}@\text{C}_{2v}(51575)\text{-C}_{84}$ is attributed to the HOMO-LUMO and (HOMO-1)-LUMO excitations together, while the first absorption peak of $\text{Sc}_2\text{O}@\text{C}_1(51580)\text{-C}_{84}$ is contributed from a combination of HOMO-LUMO and HOMO-(LUMO+1) excitations. This is quite consistent with the fact that energy-level differences between HOMO and (HOMO-1) of $\text{Sc}_2\text{O}@\text{C}_{2v}(51575)\text{-C}_{84}$ as well as LUMO and (LUMO+1) of $\text{Sc}_2\text{O}@\text{C}_1(51580)\text{-C}_{84}$ are very small (please see Figures 3, S4, and S5). Details of electronic transitions corresponding to the two peaks were collected in the Supporting Information. Consequently, the difference of the first absorption peak positions of the two $\text{Sc}_2\text{O}@\text{C}_{84}$ isomers is larger compared with the difference of their HOMO-LUMO gaps. The computed optical bandgaps of $\text{Sc}_2\text{O}@\text{C}_{2v}(51575)\text{-C}_{84}$ and $\text{Sc}_2\text{O}@\text{C}_1(51580)\text{-C}_{84}$ can be estimated to be 1.20 and 1.13 eV, respectively, in terms of their absorption onsets at 1018 and 1083 nm. Both of them are

much more blue-shifted than that of 1587 nm for the recently characterized $\text{Sc}_2\text{O}@\text{T}_d(19151)\text{-C}_{76}$ structure.²⁹ It is known that 1.0 eV is the empirical boundary of large and small bandgap fullerenes.¹ Thus, both $\text{Sc}_2\text{O}@\text{C}_{2v}(51575)\text{-C}_{84}$ and $\text{Sc}_2\text{O}@\text{C}_1(51580)\text{-C}_{84}$ can be assigned as a large bandgap metallofullerene. To the best of our knowledge, this is the first reported case of large band gap dimetal oxide clusterfullerenes.^{25,29} Their large optical bandgaps indicate that both thermodynamically stable $\text{Sc}_2\text{O}@\text{C}_{84}$ isomers also should possess great kinetic stabilities. Consequently, it is promising to synthesize them experimentally. Because of the large bandgap nature, conductivities and charge-carrier mobilities of solid $\text{Sc}_2\text{O}@\text{C}_{2v}(51575)\text{-C}_{84}$ and $\text{Sc}_2\text{O}@\text{C}_1(51580)\text{-C}_{84}$ should be poor. Thus, they may act as new insulating materials in the future. Additionally, there is a strong absorption peak at 739 nm, while a corresponding peak at 709 nm for the $\text{Sc}_2\text{O}@\text{C}_{2v}(51575)\text{-C}_{84}$ isomer is weak. They can act as fingerprint peaks for the identification of two isomers.

Since IR spectra also can aid to distinguish the structures of different isomers with the same molecular formula, we compare IR spectra of two $\text{Sc}_2\text{O}@\text{C}_{84}$ isomers. They were simulated according to the results of harmonic vibrational analysis, and were shown in Figure 9. The spectrum of either $\text{Sc}_2\text{O}@\text{C}_{2v}(51575)\text{-C}_{84}$ or $\text{Sc}_2\text{O}@\text{C}_1(51580)\text{-C}_{84}$ can be divided into three regions. A series of small peaks can be observed in the region of $0\text{--}200\text{ cm}^{-1}$, which belong to various kinds of metal cluster vibration. The wavenumbers of these vibrational modes are small due to the relatively large mass of encapsulated scandium oxide cluster. The region from 200 cm^{-1} to $\sim 920\text{ cm}^{-1}$ for $\text{Sc}_2\text{O}@\text{C}_{2v}(51575)\text{-C}_{84}$ and $\text{Sc}_2\text{O}@\text{C}_1(51580)\text{-C}_{84}$ corresponds to the breathing and rocking vibration of their

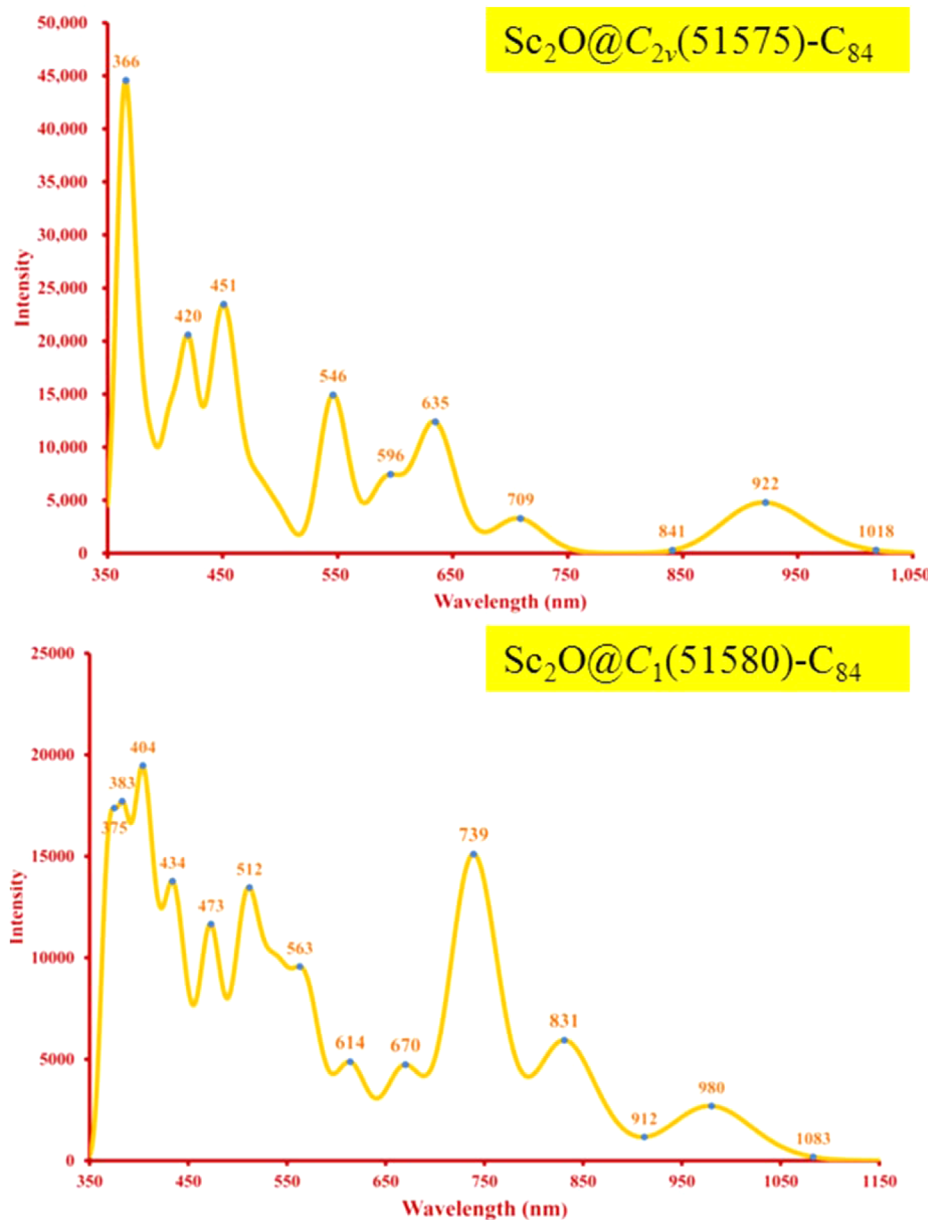


Figure 8. Simulated UV–vis–NIR spectra of Sc₂O@C_{2v}(51575)-C₈₄ and Sc₂O@C₁(51580)-C₈₄.

cages. Main IR absorptions of this vibrational mode locate in the range from 450 to 800 cm⁻¹. Specifically, two moderately strong peaks with four relatively weak ones can be observed in this region of Sc₂O@C_{2v}(51575)-C₈₄. As for the Sc₂O@C₁(51580)-C₈₄ structure, only one moderately strong absorption with two weak ones are recognized. One can notice obvious resonances between the stretch vibration of two Sc–O bonds and the breathing vibration of the C_{2v}(51575)-C₈₄ cage at wavenumbers of 731.44, 741.85, 742.46, and 745.07 cm⁻¹. Similar resonances also can be found for the Sc₂O@C₁(51580)-C₈₄ molecule at wavenumbers of 725.59, 727.54, 733.62, 744.12, and 747.08 cm⁻¹. Both Sc₂O@C₈₄ isomers show the strongest infrared absorptions in the third region that is starting from the wavenumber of ~1000 cm⁻¹, corresponding to the C–C stretching vibration of two cages. In this region, as many as 16 absorption peaks can be clearly identified for the Sc₂O@C_{2v}(51575)-C₈₄ structure, including four sharp and strong peaks as well as seven moderate ones. As for another isomer,

there are only two strong peaks with the wavenumbers of 1353.65 and 1421.19 cm⁻¹, and other infrared absorptions are much weaker. Therefore, the third region of infrared spectrum can act as fingerprint peaks for elucidating different structures of Sc₂O@C₈₄ isomers.

CONCLUSIONS

After DFT combined with statistical thermodynamic studies are applied to the recent mass spectrum detected Sc₂O@C₈₄ species, two stable isomers were uncovered unambiguously. A discandium oxide cluster is encapsulated in C_{2v}(51575)-C₈₄ and C₁(51580)-C₈₄ cage, obeying the isolated pentagon rule. Sc₂O@C_{2v}(51575)-C₈₄ possesses the lowest potential energy with the best thermodynamic abundance at relatively low-temperature region. This is the first case that an endohedral fullerene containing the C_{2v}(51575)-C₈₄ cage acts as the lowest-energy isomer. Sc₂O@C₁(51580)-C₈₄ is the third lowest-energy isomer, but its molar fraction rises rapidly with the increase of

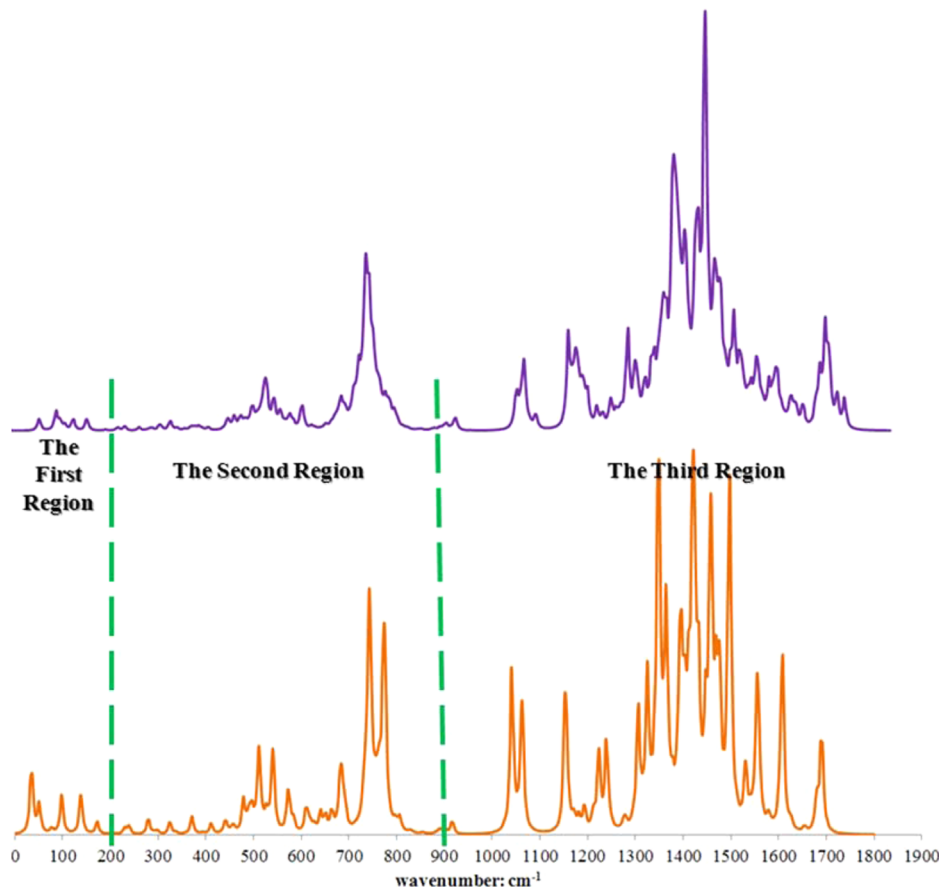


Figure 9. Simulated IR spectrum of $\text{Sc}_2\text{O}@\text{C}_{2v}(51575)\text{-C}_{84}$ (orange) and $\text{Sc}_2\text{O}@\text{C}_1(51580)\text{-C}_{84}$ (purple).

temperature. To the best of our knowledge, this is the first report of a cluster fullerene containing the $\text{C}_1(51580)\text{-C}_{84}$ cage. $\text{Sc}-\text{O}-\text{Sc}$ angles, as well as $\text{Sc}-\text{O}$ and nearest $\text{Sc}-\text{cage}$ distances, are comparable with those in the $\text{C}_s(6)\text{-C}_{82}$ cage, suggesting that a Sc_2O cluster can keep its ideal structure in both C_{84} cages. However, both cages still deform a lot after encapsulation although Sc_2O is the smallest endohedral metal cluster so far. The $\text{Sc}_2\text{O}@\text{(51575)}\text{-C}_{84}$ keeps the C_{2v} symmetry of its pristine cage, resulting in a symmetrical distribution of its HOMO. Consequently, it can be predicted that regioselectivity of nucleophilic and oxidation reactions on its cage is poor. Totally 23 peaks including 19 full-intensity peaks (four carbons) and four half-intensity peaks (two carbons) are expected in its ^{13}C NMR spectrum ranging from 124 to 153 ppm due to the C_{2v} symmetry of the whole molecule. On the contrary, the HOMO distribution of $\text{Sc}_2\text{O}@\text{C}_1(51580)\text{-C}_{84}$ is anisotropic, due to its C_1 symmetry. It is reasonable to suppose that it has good regioselectivity for the corresponding nucleophilic and oxidation reactions. Totally 84 peaks can be found in its NMR spectrum ranging from 122 to 159 ppm. Both covalent and ionic interactions coexist between a scandium atom and an oxygen one as well as a scandium atom and the fullerene cage, while the covalent interaction in both stable $\text{Sc}_2\text{O}@\text{C}_{84}$ isomers is dramatically weaker than that in the previously studied $\text{Sc}_2\text{S}@\text{C}_{68}$. It should be the most important difference between a dimetal oxide clusterfullerene and a sulfide one. UV-vis-NIR and infrared spectra of $\text{Sc}_2\text{O}@\text{(51575)}\text{-C}_{84}$ and $\text{Sc}_2\text{O}@\text{C}_1(51580)\text{-C}_{84}$ have been simulated at last. They can provide helpful methods to distinguish those two $\text{Sc}_2\text{O}@\text{C}_{84}$ isomers.

ASSOCIATED CONTENT

S Supporting Information

The Supporting Information is available free of charge on the ACS Publications website at DOI: 10.1021/acs.jpca.5b07336.

Relative energy sequence of C_{84}^{2-} anions screened at AM1 and B3LYP/6-31G(d) level; detailed process of structural determination for $\text{Sc}_2\text{O}@\text{C}_{84}$ at M06-2X functional theory; structural optimization of several $\text{Sc}_2\text{O}@\text{C}_{84}$ isomers at B3PW91 and PBE/PBE functional theory; symmetry operation of $\text{Sc}_2\text{O}@\text{C}_{2v}(51575)\text{-C}_{84}$; cage deformations and binding energies as well as electron affinity (EA) and ionization potential (IP) of two thermodynamic favorable $\text{Sc}_2\text{O}@\text{C}_{84}$ isomers; occupied frontier orbitals of two $\text{Sc}_2\text{O}@\text{C}_{84}$ isomers from (HOMO-1) to (HOMO-8); the (HOMO-8) of previously studied $\text{Sc}_2\text{S}@\text{C}_{2v}(6073)\text{-C}_{68}$; and Cartesian coordinates of $\text{Sc}_2\text{O}@\text{C}_{2v}(51575)\text{-C}_{84}$ and $\text{Sc}_2\text{O}@\text{C}_1(51580)\text{-C}_{84}$. (PDF)

AUTHOR INFORMATION

Corresponding Author

*E-mail: xzhao@mail.xjtu.edu.cn. Fax: +86 29 82668559. Phone: +86 29 82665671.

Notes

The authors declare no competing financial interest.

ACKNOWLEDGMENTS

This work has been financially supported by the National Natural Science Foundation of China (Nos. 21171138 and

21573172), the National Key Basic Research Program of China (Nos. 2011CB209404 and 2012CB720904), and the Specified Research Fund for the Doctoral Program of Higher Education of China (SRFDP No. 20130201110033). One of authors (Y.-J.G.) shows gratitude to Dr. H. Zheng for helpful discussions and also acknowledges Ms. X.-Y. Chen for the aid of illustrations.

■ REFERENCES

- (1) Popov, A. A.; Yang, S.; Dunsch, L. Endohedral Fullerenes. *Chem. Rev.* **2013**, *113*, 5989–6113.
- (2) Yamada, M.; Kurihara, H.; Suzuki, M.; Guo, J.-D.; Waelchli, M.; Olmstead, M. M.; Balch, A. L.; Nagase, S.; Maeda, Y.; Hasegawa, T.; Lu, X.; Akasaka, T. $\text{Sc}_2@\text{C}_{66}$ Revisited: An Endohedral Fullerene with scandium Ions Nestled within Two Unsaturated Linear Triquinanes. *J. Am. Chem. Soc.* **2014**, *136*, 7611–7614.
- (3) Zhang, Y.; Ghiasi, K. B.; Deng, Q.; Samoylova, N. A.; Olmstead, M. M.; Balch, A. L.; Popov, A. A. Synthesis and Structure of $\text{LaSc}_2\text{N}@\text{C}_s(\text{hept})-\text{C}_{80}$ with One Heptagon and Thirteen Pentagons. *Angew. Chem.* **2015**, *127*, 505–509.
- (4) Popov, A. A.; Zhang, L.; Dunsch, L. A. Pseudoatom in a Cage: Trimallofullerene $\text{Y}_3@\text{C}_{80}$ Mimics $\text{Y}_3\text{N}@\text{C}_{80}$ with Nitrogen Substituted by a Pseudoatom. *ACS Nano* **2010**, *4*, 795–802.
- (5) Akasaka, T.; Wudl, F.; Nagase, S. *Chemistry of Nanocarbons*; Wiley-Blackwell: London, U.K., 2010.
- (6) Akasaka, T.; Nagase, S. *Endofullerenes: A New Family of Carbon Clusters*; Kluwer Academic Publisher: Dordrecht, The Netherlands, 2002.
- (7) Dunsch, L.; Yang, S. Metal Nitride Cluster Fullerenes: Their Current State and Future Prospects. *Small* **2007**, *3*, 1298–1320.
- (8) Lu, X.; Akasaka, T.; Nagase, S. Chemistry of Endohedral Metallofullerenes: The Role of Metals. *Chem. Commun.* **2011**, *47*, 5942–5957.
- (9) Lu, X.; Akasaka, T.; Nagase, S. Carbide Cluster Metallofullerenes: Structure, Properties, and Possible Origin. *Acc. Chem. Res.* **2013**, *46*, 1627–1635.
- (10) Lu, X.; Feng, L.; Akasaka, T.; Nagase, S. Current Status and Future Developments of Endohedral Metallofullerenes. *Chem. Soc. Rev.* **2012**, *41*, 7723–7760.
- (11) Dorn, H. C.; Rice, G.; Glass, T.; Harich, K.; Cromer, F.; Jordan, M. R.; Craft, J.; Hadju, E.; Bible, R.; Olmstead, M. M.; Maitra, K.; Fisher, A. J.; Balch, A. L.; Stevenson, S. Small-Bandgap Endohedral Metallofullerene in High Yield and Purity. *Nature* **1999**, *401*, 55–57.
- (12) Wang, C. R.; Kai, T.; Tomiyama, T.; Yoshida, T.; Kobayashi, Y.; Nishibori, E.; Takata, M.; Sakata, M.; Shinohara, H. A Scandium Carbide Endohedral Metallofullerene: $(\text{Sc}_2\text{C}_2)@\text{C}_{84}$. *Angew. Chem., Int. Ed.* **2001**, *40*, 397–399.
- (13) Inoue, T.; Tomiyama, T.; Sugai, T.; Okazaki, T.; Suematsu, T.; Fujii, N.; Utsumi, H.; Nojima, K.; Shinohara, H. Trapping a C_2 Radical in Endohedral Metallofullerenes: Synthesis and Structures of $(\text{Y}_2\text{C}_2)@\text{C}_{82}$ (Isomers I, II, and III). *J. Phys. Chem. B* **2004**, *108*, 7573–7579.
- (14) Yang, H.; Lu, C.; Liu, Z.; Jin, H.; Che, Y.; Olmstead, M. M.; Balch, A. L. Detection of a Family of Gadolinium-Containing Endohedral Fullerenes and the Isolation and Crystallographic Characterization of One Member as a Metal – Carbide Encapsulated inside a Large Fullerene Cage. *J. Am. Chem. Soc.* **2008**, *130*, 17296–17300.
- (15) Li, F.-F.; Chen, N.; Mulet-Gas, M.; Triana, V.; Murillo, J.; Rodríguez-Fortea, A.; Poblet, J. M.; Echegoyen, L. $\text{Ti}_2\text{S}@\text{D}_{3h}(2410)-\text{C}_{78}$: a Sulfide Cluster Metallofullerene Containing Only Transition Metals inside the Cage. *Chem. Sci.* **2013**, *4*, 3404–3410.
- (16) Yang, T.; Zhao, X.; Nagase, S. Quantum Chemical Insight of the Dimetallic Sulfide Endohedral Fullerene $\text{Sc}_2\text{S}@\text{C}_{70}$: Does It Possess the Conventional D_{3h} Cage? *Chem. - Eur. J.* **2013**, *19*, 2649–2654.
- (17) Guo, Y.-J.; Gao, B.-C.; Yang, T.; Nagase, S.; Zhao, X. $\text{Sc}_2\text{S}@\text{C}_{68}$: an Obtuse Di-Scandium Sulfide Cluster Trapped in a C_{2v} Fullerene Cage. *Phys. Chem. Chem. Phys.* **2014**, *16*, 15994–16002.
- (18) Wang, T.-S.; Feng, L.; Wu, J.-Y.; Xu, W.; Xiang, J.-F.; Tan, K.; Ma, Y.-H.; Zheng, J.-P.; Jiang, L.; Lu, X.; Shu, C.-Y.; Wang, C.-R. Planar Quinary Cluster inside a Fullerene Cage: Synthesis and Structural Characterization of $\text{Sc}_3\text{NC}@\text{C}_{80}-I_h$. *J. Am. Chem. Soc.* **2010**, *132*, 16362–16364.
- (19) Yang, S.; Chen, C.; Liu, F.; Xie, Y.; Li, F.; Jiao, M.; Suzuki, M.; Wei, T.; Wang, S.; Chen, Z.; Lu, X.; Akasaka, T. An Improbable Monometallic Cluster Entrapped in a Popular Fullerene Cage: $\text{YCN}@\text{C}_s(6)-\text{C}_{82}$. *Sci. Rep.* **2013**, *3*, 01487–1–01487–5.
- (20) Liu, F.; Wang, S.; Guan, J.; Wei, T.; Zeng, M.; Yang, S. Putting a Terbium-Monometallic Cyanide Cluster into the C_{82} Fullerene Cage: $\text{TbCN}@\text{C}_2(\text{S})-\text{C}_{82}$. *Inorg. Chem.* **2014**, *53*, 5201–5205.
- (21) Zheng, H.; Zhao, X.; He, L.; Wang, W.-W.; Nagase, S. Quantum Chemical Determination of Novel C_{82} Monometallofullerenes Involving a Heterogeneous Group. *Inorg. Chem.* **2014**, *53*, 12911–12917.
- (22) Mercado, B.; Olmstead, M. M.; Beavers, C. M.; Easterling, M. L.; Stevenson, S.; Mackey, M. A.; Coumbe, C. E.; Phillips, J. D.; Phillips, J. P.; Poblet, J. P.; Balch, A. L. A Seven Atom Cluster in a Carbon Cage, the Crystallographically Determined Structure of $\text{Sc}_4(\mu_3\text{-O})_3@I_h-\text{C}_{80}$. *Chem. Commun.* **2010**, *46*, 279–281.
- (23) Stevenson, S.; Mackey, M. A.; Stuart, M. A.; Phillips, J. P.; Easterling, M. L.; Chancellor, C. J.; Olmstead, M. M.; Balch, A. L. A Distorted Tetrahedral Metal Oxide Cluster inside an Icosahedral Carbon Cage. Synthesis, Isolation, and Structural Characterization of $\text{Sc}_4(\mu_3\text{-O})_2@I_h-\text{C}_{80}$. *J. Am. Chem. Soc.* **2008**, *130*, 11844–11845.
- (24) Mercado, B. Q.; Stuart, M. A.; Mackey, M. A.; Pickens, J. E.; Confait, B. S.; Stevenson, S.; Easterling, M. L.; Valencia, R.; Rodríguez-Fortea, A.; Poblet, J. M.; Olmstead, M. M.; Balch, A. L. $\text{Sc}_2(\mu_2\text{-O})$ Trapped in a Fullerene Cage: The Isolation and Structural Characterization of $\text{Sc}_2(\mu_2\text{-O})@\text{C}_s(6)-\text{C}_{82}$ and the Relevance of the Thermal and Entropic Effects in Fullerene Isomer Selection. *J. Am. Chem. Soc.* **2010**, *132*, 12098–12105.
- (25) Zhang, M.; Hao, Y.; Li, X.; Feng, L.; Yang, T.; Wan, Y.; Chen, N.; Slanina, Z.; Uhlík, F.; Cong, H. Facile Synthesis of an Extensive Family of $\text{Sc}_2\text{O}@\text{C}_{2n}$ ($n = 35 – 47$) and Chemical Insight into the Smallest Member of $\text{Sc}_2\text{O}@\text{C}_2(7892)-\text{C}_{70}$. *J. Phys. Chem. C* **2014**, *118*, 28883–28889.
- (26) Alegret, N.; Abella, L.; Rodríguez-Fortea, A.; Poblet, J. M. Cubane Oxides inside Middle-sized Fullerenes: the Next Endohedrals to be Detected? *Theor. Chem. Acc.* **2015**, *134*, 15.
- (27) Chen, N.; Chaur, M. N.; Moore, C.; Pinzón, J. R.; Valencia, R.; Rodríguez-Fortea, A.; Poblet, J. M.; Echegoyen, L. Synthesis of a New Endohedral Fullerene Family, $\text{Sc}_2\text{S}@\text{C}_{2n}$ ($2n = 40 - 50$) by the Introduction of SO_2 . *Chem. Commun.* **2010**, *46*, 4818–4820.
- (28) Chen, N.; Beavers, C. M.; Mulet-Gas, M.; Rodríguez-Fortea, A.; Munoz, E. J.; Li, Y.-Y.; Olmstead, M. M.; Balch, A. L.; Poblet, J. M.; Echegoyen, L. $\text{Sc}_2\text{S}@\text{C}_s(10528)-\text{C}_{72}$: A Dimetallic Sulfide Endohedral Fullerene with a Non Isolated Pentagon Rule Cage. *J. Am. Chem. Soc.* **2012**, *134*, 7851–7860.
- (29) Yang, T.; Hao, Y.; Abella, L.; Tang, Q.; Li, X.; Wan, Y.; Rodríguez-Fortea, A.; Poblet, J. M.; Feng, L.; Chen, N. $\text{Sc}_2\text{O}@\text{T}_d(19151)-\text{C}_{76}$: Hindered Cluster Motion inside a Tetrahedral Carbon Cage Probed by Crystallographic and Computational Studies. *Chem. - Eur. J.* **2015**, *21*, 11110.
- (30) Lu, X.; Slanina, Z.; Akasaka, T.; Tsuchiya, T.; Mizorogi, N.; Nagase, S. $\text{Yb}@\text{C}_{2n}$ ($n = 40, 41, 42$): New Fullerene Allotropes with Unexplored Electrochemical Properties. *J. Am. Chem. Soc.* **2010**, *132*, 5896–5905.
- (31) Zhang, W.; Suzuki, M.; Xie, Y.; Bao, L.; Cai, W.; Slanina, Z.; Nagase, S.; Xu, M.; Akasaka, T.; Lu, X. Molecular Structure and Chemical Property of a Divalent Metallofullerene $\text{Yb}@\text{C}_2(13)-\text{C}_{84}$. *J. Am. Chem. Soc.* **2013**, *135*, 12730–12735.
- (32) Yang, H.; Yu, M.; Jin, H.; Liu, Z.; Yao, M.; Liu, B.; Olmstead, M. M.; Balch, A. L. Isolation of Three Isomers of $\text{Sm}@\text{C}_{84}$ and X-ray Crystallographic Characterization of $\text{Sm}@\text{D}_{3d}(19)-\text{C}_{84}$ and $\text{Sm}@\text{C}_2(13)-\text{C}_{84}$. *J. Am. Chem. Soc.* **2012**, *134*, 5331–5338.
- (33) Kurihara, H.; Lu, X.; Iiduka, Y.; Nikawa, H.; Hachiya, M.; Mizorogi, N.; Slanina, Z.; Tsuchiya, T.; Nagase, S.; Akasaka, T. X-ray

- Structures of Sc_2C_{2n} ($n = 40-42$): In-Depth Understanding of the Core-Shell Interplay in Carbide Cluster Metallofullerenes. *Inorg. Chem.* **2012**, *51*, 746–750.
- (34) Yang, T.; Zhao, X.; Li, S.-T.; Nagase, S. Is the Isolated Pentagon Rule Always Satisfied for Metallic Carbide Endohedral Fullerenes? *Inorg. Chem.* **2012**, *51*, 11223–11225.
- (35) Zhang, J.; Bowles, F. L.; Bearden, D. W.; Ray, W. K.; Fuhrer, T.; Ye, Y.; Dixon, C.; Harich, K.; Helm, R. F.; Olmstead, M. M.; Balch, A. L.; Dorn, H. C. A Missing Link in the Transformation from Asymmetric to Symmetric Metallofullerene Cages Implies a Top-Down Fullerene Formation Mechanism. *Nat. Chem.* **2013**, *5*, 880–885.
- (36) Beavers, C. M.; Zuo, T.; Duchamp, J. C.; Harich, K.; Dorn, H. C.; Olmstead, M. M.; Balch, A. L. $\text{Tb}_3\text{N}@\text{C}_{84}$: An Improbable, Egg-Shaped Endohedral Fullerene that Violates the Isolated Pentagon Rule. *J. Am. Chem. Soc.* **2006**, *128*, 11352–11353.
- (37) Zuo, T.; Walker, K.; Olmstead, M. M.; Melin, F.; Holloway, B. C.; Echegoyen, L.; Dorn, H. C.; Chaur, M. N.; Chancellor, C. J.; Beavers, C. M.; Balch, A. L.; Athans, A. J. New Egg-Shaped Fullerenes: Non-Isolated Pentagon Structures of $\text{Tm}_3\text{N}@\text{C}_s(51365)-\text{C}_{84}$ and $\text{Gd}_3\text{N}@\text{C}_s(51365)-\text{C}_{84}$. *Chem. Commun.* **2008**, 1067–1069.
- (38) Burke, B. G.; Chan, J.; Williams, K. A.; Ge, J.; Shu, C.; Fu, W.; Dorn, H. C.; Kushmerick, J. G.; Puretzky, A. A.; Geohegan, D. B. Investigations of $\text{Gd}_3\text{N}@\text{C}_{2n}$ ($40 \leq n \leq 44$) Family by Raman and Inelastic Electron Tunneling Spectroscopy. *Phys. Rev. B: Condens. Matter Mater. Phys.* **2010**, *81*, 115423.
- (39) Fu, W.; Xu, L.; Azurmendi, H.; Ge, J.; Fuhrer, T.; Zuo, T.; Reid, J.; Shu, C.; Harich, K.; Dorn, H. C. ^{89}Y and ^{13}C NMR Cluster and Carbon Cage Studies of an Yttrium Metallofullerene Family, $\text{Y}_3\text{N}@\text{C}_{2n}$ ($n = 40-43$). *J. Am. Chem. Soc.* **2009**, *131*, 11762–11769.
- (40) Zhao, C.; Lei, D.; Gan, L.-H.; Zhang, Z.-X.; Wang, C.-R. Theoretical Study on Experimentally Detected $\text{Sc}_2\text{S}@\text{C}_{84}$. *ChemPhysChem* **2014**, *15*, 2780–2784.
- (41) Fowler, P. W.; Manolopoulos, D. E. *An Atlas of Fullerenes*; Oxford University Press: Oxford, U.K., 1995.
- (42) Zhao, P.; Yang, T.; Guo, Y.-J.; Dang, J.-S.; Zhao, X.; Nagase, S. Dimetallic Sulfide Endohedral Metallofullerene $\text{Sc}_2\text{S}@\text{C}_{76}$: Density Functional Theory Characterization. *J. Comput. Chem.* **2014**, *35*, 1657–1663.
- (43) Takata, M.; Nishibori, E.; Umeda, B.; Sakata, M.; Yamamoto, E.; Shinohara, H. Structural of Endohedral Dimetallofullerene $\text{Sc}_2@\text{C}_{84}$. *Phys. Rev. Lett.* **1997**, *78*, 3330–3333.
- (44) Krause, M.; Hulman, M.; Kuzmany, H.; Dennis, T. J. S.; Inakuma, M.; Shinohara, H. Diatomic Metal Encapsulates in Fullerene Cages: A Raman and Infrared Analysis of C_{84} and $\text{Sc}_2@\text{C}_{84}$ with D_{2d} Symmetry. *J. Chem. Phys.* **1999**, *111*, 7976–7984.
- (45) Zheng, H.; Zhao, X.; Wang, W.-W.; Yang, T.; Nagase, S. $\text{Sc}_2@\text{C}_{70}$ rather than $\text{Sc}_2\text{C}_2@\text{C}_{68}$: Density Functional Theory Characterization of Metallofullerene Sc_2C_{70} . *J. Chem. Phys.* **2012**, *137*, 014308.
- (46) Becke, A. Density-Functional Exchange-Energy Approximation with Correct Asymptotic Behavior. *Phys. Rev. A: At., Mol., Opt. Phys.* **1988**, *38*, 3098–3100.
- (47) Becke, A. D. Density-Functional Thermochemistry. III. The Role of Exact Exchange. *J. Chem. Phys.* **1993**, *98*, 5648–5652.
- (48) Lee, C.; Yang, W.; Parr, R. G. Development of the Colle-Salvetti Correlation-Energy Formula into a Functional of the Electron Density. *Phys. Rev. B: Condens. Matter Mater. Phys.* **1988**, *37*, 785–789.
- (49) Zhao, Y.; Schultz, N. E.; Truhlar, D. G. Design of Density Functionals by Combining the Method of Constraint Satisfaction with Parametrization for Thermochemical kinetics, and Noncovalent Interactions. *J. Chem. Theory Comput.* **2006**, *2*, 364–382.
- (50) Hay, P. J.; Wadt, W. R. Ab initio Effective Core Potentials for Molecular Calculations: Potentials for the Transition Metal Atoms Sc to Hg. *J. Chem. Phys.* **1985**, *82*, 270–283.
- (51) Perdew, J. P.; Wang, Y. Accurate and Simple Analytic Representation of the Electron-Gas Correlation Energy. *Phys. Rev. B: Condens. Matter Mater. Phys.* **1992**, *45*, 13244–13249.
- (52) Perdew, J. P.; Burke, K.; Ernzerhof, M. Generalized Gradient Approximation Made Simple. *Phys. Rev. Lett.* **1996**, *77*, 3865–3868.
- (53) Slanina, Z.; Lee, S.-L.; Uhlík, F.; Adamowicz, L.; Nagase, S. Computing Relative Stabilities of Metallofullerenes by Gibbs Energy Treatments. *Theor. Chem. Acc.* **2007**, *117*, 315–322.
- (54) Tomasi, J.; Mennucci, B.; Cammi, R. Quantum Mechanical Continuum Solvent Models. *Chem. Rev.* **2005**, *105*, 2999–3094.
- (55) Sun, G.; Kertesz, M. Theoretical ^{13}C NMR Spectra of IPR Isomers of Fullerenes C_{60} , C_{70} , C_{72} , C_{74} , C_{76} , and C_{78} Studied by Density Functional Theory. *J. Phys. Chem. A* **2000**, *104*, 7398–7403.
- (56) Frisch, M. J.; Trucks, G. W.; Schlegel, H. B.; Scuseria, G. E.; Robb, M. A.; Cheeseman, J. R.; Scalmani, G.; Barone, V.; Mennucci, B.; Petersson, G. A.; Nakatsuji, H.; Caricato, M.; Li, X.; Hratchian, H. P.; Izmaylov, A. F.; Bloino, J.; Zheng, G.; Sonnenberg, J. L.; Hada, M.; Ehara, M.; Toyota, K.; Fukuda, R.; Hasegawa, J.; Ishida, M.; Nakajima, T.; Honda, Y.; Kitao, O.; Nakai, H.; Vreven, T.; Montgomery, J. A., Jr.; Peralta, J. E.; Ogliaro, F.; Bearpark, M.; Heyd, J. J.; Brothers, E.; Kudin, K. N.; Staroverov, V. N.; Kobayashi, R.; Normand, J.; Raghavachari, K.; Rendell, A. J.; Burant, C.; Iyengar, S. S.; Tomasi, J.; Cossi, M.; Rega, N.; Millam, J. M.; Klene, M.; Knox, J. E.; Cross, J. B.; Bakken, V.; Adamo, C.; Jaraillo, J.; Comperts, R.; Stratmann, R. E.; Yazeyev, O.; Austin, A. J.; Cammi, R.; Pomelli, C.; Ochterski, J. W.; Martin, R. L.; Morokuma, K.; Zakrzewski, V. G.; Voth, G. A.; Salvador, P.; Dannenberg, J. J.; Dapprich, S.; Daniels, A. D.; Farkas, Ö.; Foresman, J. B.; Ortiz, J. V.; Cioslowski, J.; Fox, D. J.; Gaussian 09, Revision A.01; Gaussian, Inc: Wallingford, CT, 2009.
- (57) Yang, T.; Zhao, X.; Nagase, S. Di-lanthanide Encapsulated into Larger Fullerene C_{100} : A DFT Survey. *Phys. Chem. Chem. Phys.* **2011**, *13*, 5034–5037.
- (58) Yang, T.; Zhao, X.; Ōsawa, E. Can a Metal-Metal Bond Hop in the Fullerene Cage? *Chem. - Eur. J.* **2011**, *17*, 10230–10234.
- (59) Guo, Y.-J.; Yang, T.; Nagase, S.; Zhao, X. Carbide Clusterfullerene $\text{Gd}_2\text{C}_2@\text{C}_{92}$ vs. Dimetallofullerene $\text{Gd}_2@\text{C}_{94}$: A Quantum Chemical Survey. *Inorg. Chem.* **2014**, *53*, 2012–2021.
- (60) Zheng, H.; Zhao, X.; Wang, W.-W.; Dang, J.-S.; Nagase, S. Quantum Chemical Insight into Metallofullerenes M_2C_{98} : $\text{M}_2\text{C}_2@\text{C}_{96}$ or $\text{M}_2@\text{C}_{98}$? Which will Survive? *J. Phys. Chem. C* **2013**, *117*, 25195–25204.
- (61) Zhang, J.; Fuhrer, T.; Fu, W.; Ge, J.; Bearden, D. W.; Dallas, J.; Duchamp, J.; Walker, K.; Champion, H.; Azurmendi, H.; Harich, K.; Dorn, H. C. Nanoscale Fullerene Compression of an Yttrium Carbide Cluster. *J. Am. Chem. Soc.* **2012**, *134*, 8487–8493.
- (62) Mercado, B. Q.; Chen, N.; Rodríguez-Fortea, A.; Mackey, M. A.; Stevenson, S.; Echegoyen, L.; Poblet, J. M.; Olmstead, M. M.; Balch, A. L. The Shape of the $\text{Sc}_2(\mu_2\text{-S})$ Unit Trapped in C_{82} : Crystallographic, Computational, and Electrochemical Studies of the Isomers, $\text{Sc}_2(\mu_2\text{-S})@\text{C}_s(6)-\text{C}_{82}$ and $\text{Sc}_2(\mu_2\text{-S})@\text{C}_s(8)-\text{C}_{82}$. *J. Am. Chem. Soc.* **2011**, *133*, 6752–6760.
- (63) Lu, T.; Chen, F. Multiwfn: A Multifunctional Wavefunction Analyzer. *J. Comput. Chem.* **2012**, *33*, 580–592.
- (64) Silvi, B.; Savin, A. Classification of Chemical Bonds Based on Topological Analysis Electron Localization Function. *Nature* **1994**, *371*, 683–686.
- (65) Savin, A.; Nesper, R.; Wengert, S.; Fassler, T. F. ELF: The Electron Localization Function. *Angew. Chem., Int. Ed. Engl.* **1997**, *36*, 1808–1832.
- (66) Kohout, M.; Wagner, F. R.; Grin, Y. Electron Localization Function for Transition-Metal Compounds. *Theor. Chem. Acc.* **2002**, *108*, 150–156.
- (67) Mayer, I. *J. Comput. Chem.* **2007**, *28*, 204–221.